Submitted draft

A Spectralon BRF data base for MISR calibration applications

Carol Bruegge, Nadine Chrien, David Haner

Jet Propulsion Laboratory, California Institute of Technology, Pasadena, California

The Multi-angle Imaging SpectroRadiometer (MISR) is an Earth observing sensor which will provide global retrievals of aerosols, clouds, and land surface parameters. Instrument specifications require high accuracy absolute calibration, as well as accurate camera-to-camera, band-to-band and pixel-to-pixel relative response determinations. In order to achieve these requirements, MISR will make use of an on-board calibrator (OBC), as well as vicarious calibration experiments. The OBC makes use of two Spectralon diffuse panels in order to provide a flat-field illumination. Monthly deployments of these panels into the camera fields-of-view will be made. At these times solar-reflected radiance values are measured by photodiode detector standards. Accurate relative bi-directional reflectance factor (BRF) data are required to transfer these photodiode measured radiances into camera-incident values. An independent calibration pathway, known as vicarious calibration, will also be implemented in order to reduce systematic errors and to provide a cross-check on the OBC findings. Here the top-of-atmosphere radiances are computed from in-situ observations of surface reflectance and atmospheric transmittances. Key to these measurements is knowledge of the hemispheric-directional reflectance factor (HDRF) of the field reflectance standards. This report describes the BRF measurements of the MISR flight panels, and provides an estimation as to the differences between HDRF and BRF for the MISR view angles. This BRF data base is available from the MISR web site.

INTRODUCTION

Spectralon is a sintered polytetrafluoroethylene (PTFE) material manufactured by Labsphere, Inc. Spectralon panels are valued as reflectance standards in that they approach Lambertian behavior, particularly at near-nadir illumination angles, are nearly spectrally neutral (Labsphere, 1998) across the visible and near infrared, and are machinable, weather-resistant and washable. For these reasons Spectralon is widely used in field validation experiments conducted in support of a remote sensing systems. More recently the material has been space qualified (Bruegge, Stiegman, et al., 1993), and has been built into the MISR on-board calibrator. Spectralon panels are also utilized on another EOS-AM1 instrument, the Moderate-Resolution Imaging Spectroradiometer (MODIS). Of those instruments who have built or propose to make use of Spectralon on-orbit, only the M.... (MOS) instrument has been launched to date. This team reports success in its flight calibration (Sümnich et al., 1977).

Address correspondence to Carol Bruegge, JPL MS 169-237, 4800 Oak Grove Dr., Pasadena, CA 91109.
Revision date December 2, 1998 4:46 pm.

Few facilities have the capability to accurately measure BRF. For this reason many have explored the suitability of a general calibration model for Spectralon (Jackson et al., 1992; Weidner and Hsia, 1981). Those that do have the capability of making BRF measurements typically quote principal plane measurements (Barnes et al., 1998; Early et al., 1999), or those for a nadir viewing sensor. (The principal plane contains the source and view-angle directions). Only one other literature report describes the BRF at all viewing angles (Feng et al., 1993). MISR, with its extreme range of viewing angles, requires such a complete mapping of BRF into the reflecting hemisphere.

Reflectance nomenclature

Following the nomenclature of Nicodemus (1977), MISR will retrieve the bidirectional reflectance-distribution factor (BRF), written

$$R(\theta_i,\phi_i;\theta_r,\phi_r)=d\Theta_r/d\Theta_{r,ideal}\,. \tag{1}$$

That is, for an irradiance incident at angle θ_i,ϕ_i, the reflected flux in view angle direction θ_r,ϕ_r is measured. This is ratioed to the flux from an ideal (lossless), perfectly diffuse (Lambertian) surface irradiated in exactly the same way as the sample. Partial derivatives are used in the notation, signifying measurement over surface element dA. The BRF is an appropriate descriptor of the reflectance under point-source, narrow-cone beam illumination. It is thus suitable for direct use in MISR on-orbit calibration, where panel illumination occurs outside the Earth's atmosphere.

Throughout this paper, all quantities associated with the incident radiation have a subscript i, and all quantities associated with reflected flux have subscript r. Reflectances will also be defined such that $\phi_i=0°$, hence reference to the illumination azimuth is subsequently omitted. For the reflected beam, $\phi_r=0°$ represents the backscattered direction and $\phi_r=180°$ represents the forward scattered direction.

Expanding the numerator and denominator in Eqn. (1) gives

$$d\Theta_r=dA\; L_r(\theta_r,\phi_r)\cos\theta_r\, d\omega_r\,, \tag{2}$$

and

$$d\Theta_{r,ideal}=dA\;[E_i(\theta_i)/\pi]\cos\theta_r\, d\omega_r\,. \tag{3}$$

Eqn. (3) comes about since the ideal diffuse surface reflects the same radiance, $E_i(\theta_i)/\pi$, in all view directions. Combining these produces

$$R(\theta_i;\theta_r,\phi_r)=L_r(\theta_r,\phi_r)\,\pi/\,E_i(\theta_i)\,. \tag{4}$$

For use in field applications, the incident irradiance consists of a mixture of solar (direct) and non-isotropic diffuse illumination. For this case we utilize the hemispherical/ directional

reflectance factor (HDRF). This is still derived from Eqn. (1) and Eqn. (4), however the reflected radiance is integrated over the reflecting hemisphere. We write

$$d\Theta_r = dA\int L_r(\theta_r,\phi_r)\cos\theta_r d\omega_r \tag{5}$$

$$= \frac{dA}{\pi}[R(\theta_o;\theta_r,\phi_r)E_{dir}(\theta_o) + \int R(\theta_i,\phi_i;\theta_r,\phi_r)L_{dif}(\theta_i,\phi_i)\cos\theta_r d\omega] \tag{6}$$

$$d\Theta_{r,\,ideal} = dAE_{tot}\int \cos\theta_r d\omega_r/\pi = dAE_{tot} \tag{7}$$

where

$$E_{dif} = \int L_{dif}(\theta_i,\phi_i)d\omega_i\,, \tag{8}$$

$$E_{tot}=E_{dir}+E_{dif}\,. \tag{9}$$

Thus,

$$r(2\pi;\theta_r,\phi_r) = \frac{1}{\pi E_{tot}}[R(\theta_o;\theta_r,\phi_r)E_{dir}(\theta_o) + \int R(\theta_i,\phi_i;\theta_r,\phi_r)L_{dif}(\theta_i,\phi_i)\cos\theta_r d\omega] \tag{10}$$

Note our usage of $R(\theta_i;\theta_r,\phi_r)$ for BRF and $r(2\pi;\theta_r,\phi_r)$ for HDRF, E_{dir}, E_{dif}, and E_{tot} for the direct, diffuse, and total downwelling incident irradiances, and θ_o for the solar incident angle. The irradiance components are those incident upon a horizontal surface and thus includes the $\cos\theta_i$ term of illumination.

The final quantity discussed in this paper is the directional/ hemispheric reflectance (DHR). Unlike the previous two quantities, the DHR is not a measure of flux ratioed to an ideal diffuser. Rather, this parameter represents the flux ratio of light reflected into a hemisphere, when the target is illuminated with a narrow cone of light from direction θ_i, to the incident flux. It is written as

$$\rho(\theta_i;2\pi) = \frac{d\int L_r(\theta_r,\phi_r)\cos\theta_r d\omega_r}{dE_i(\theta_i)} = (d\int R(\theta_i,\phi_i;\theta_r,\phi_r)\cos\theta_r d\omega_r)/\pi \tag{11}$$

For this equation the reflected radiance was substituted using Eqn. (4).

MISR EXPERIMENT

As part of the Earth Observing System (EOS) mission, NASA plans to launch a series of platforms beginning in 1999. The first of these will include instruments to measure geophysical parameters used in the study of the terrestrial surface, atmospheric composition, clouds, aerosols,

and radiation balance. The Multi-angle Imaging SpectroRadiometer (MISR) instrument (Diner et al., 1998) has been selected for flight on the initial platform, designated EOS-AM1. Absolute radiometric calibration is to be maintained to within 3% uncertainty throughout the mission. Due to this challenging requirement an on-board calibration (OBC) subsystem has been designed as part of the instrument. Elements include a pair of diffuse reflectance standard panels that will be deployed at monthly intervals to reflect solar irradiance into the MISR cameras. Absolute reflectance knowledge of the panels is not required, as MISR makes use of on-board detector standards to establish the radiometric scale. As the cameras and photodiode standards are not co-aligned, relative changes in radiance, reflected in the direction of the cameras as compared to that in the direction of the photodiodes, is required. For this transfer MISR requires accuracy only in the relative BRF of the panels.

MISR has been designed and built by the Jet Propulsion Laboratory (JPL). It utilizes nine cameras which image the earth in a pushbroom fashion. The cameras are arranged with one nadir camera and two banks of four cameras pointing in the forward and aftward directions with respect to the spacecraft ground track. Images are acquired at the Earth's surface with view angles of 0°, ±26.1°, ±45.6°, ±60.0°, and ±70.5°. Radiometrically calibrated images at each angle will be obtained at the four spectral bands 446, 558, 672, and 866 nm. The nine cameras are designated An, Af/Aa, Bf/Ba, Cf/Ca, and Df/Da. Here "A" through "D" denote one of four camera designs, ranging from the small (including nadir) to large view angle configurations. Additionally, "f" denotes a forward pointing camera, "a" an aftward pointing camera, and "n" the nadir camera.

MISR radiometric calibration requirements are given in Table 1, as specified at the 68% (1σ) confidence level. The absolute calibration goal refers to the transfer of instrument output digital numbers (DN) into incident radiance values, traceable to Système International (SI) units (Meyer-Arendt, 1968). High accuracy is required for long-term monitoring programs, and to enable change detection. The relative calibration requirements are needed for accurate determination of angular signatures, which in turn enable aerosol retrievals and BRF determination of clouds and surface scenes. In this table the requirements are defined at two equivalent reflectance levels, ρ_{eq}, where the equivalent reflectance is defined to be the measured radiance divided by E_o/π, and where E_o is the exo-atmospheric irradiance weighted by the MISR spectral response function. In addition to these requirements, those such as stability and signal-to-noise have been defined and are equally critical (Bruegge, Duval et al., 1993).

Table 1. MISR radiometric calibration requirements

Parameter	Requirement at ρ_{eq}=1.0	Requirement at ρ_{eq}=0.5
Absolute	±3%	±6%

Table 1. MISR radiometric calibration requirements

Parameter	Requirement at ρ_{eq}=1.0	Requirement at ρ_{eq}=0.5
Camera relative	±1%	±2%
Band relative	±1%	±2%
Pixel relative	±0.5%	±1%

On-board calibrator overview

The MISR calibration panels are required to be made from a material that has a high, near-Lambertian reflectance. While not in use the panels are stowed and protected by a labyrinth seal. At approximately monthly time intervals the panels are deployed for calibration. Figure 1 shows the nine MISR cameras, with the North Pole panel deployed for calibration. Over the North Pole, this plate will swing aftward to diffusely reflect sunlight into the fields-of-view of the aftward-looking and nadir cameras. Over the South Pole, the other plate will swing forward for calibration of the forward-looking cameras. The nadir camera will view both panels, providing a link between the two sets of observations. The two panels are required to support the fore- and aft-camera views, and South/ North observation periods are required to achieve solar illumination of the two panels respectively. The panels are deployed through an angle of 67.5°, and receive solar illumination at about 45° from nadir. At this geometry the specular direction will fall mid-way between the B and C cameras, thereby minimizing departures from Lambertian reflectance. (This was a precautionary measure as no specular reflection component has in practice been observed). Cumulative space exposure time (deploy time) for each panel is expected to be no more than 100 hours over the mission life. Flight qualification testing has verified panel reflectance stability (Bruegge, Stiegman, et al., 1993; Stiegman, Bruegge, and Springsteen, 1993).

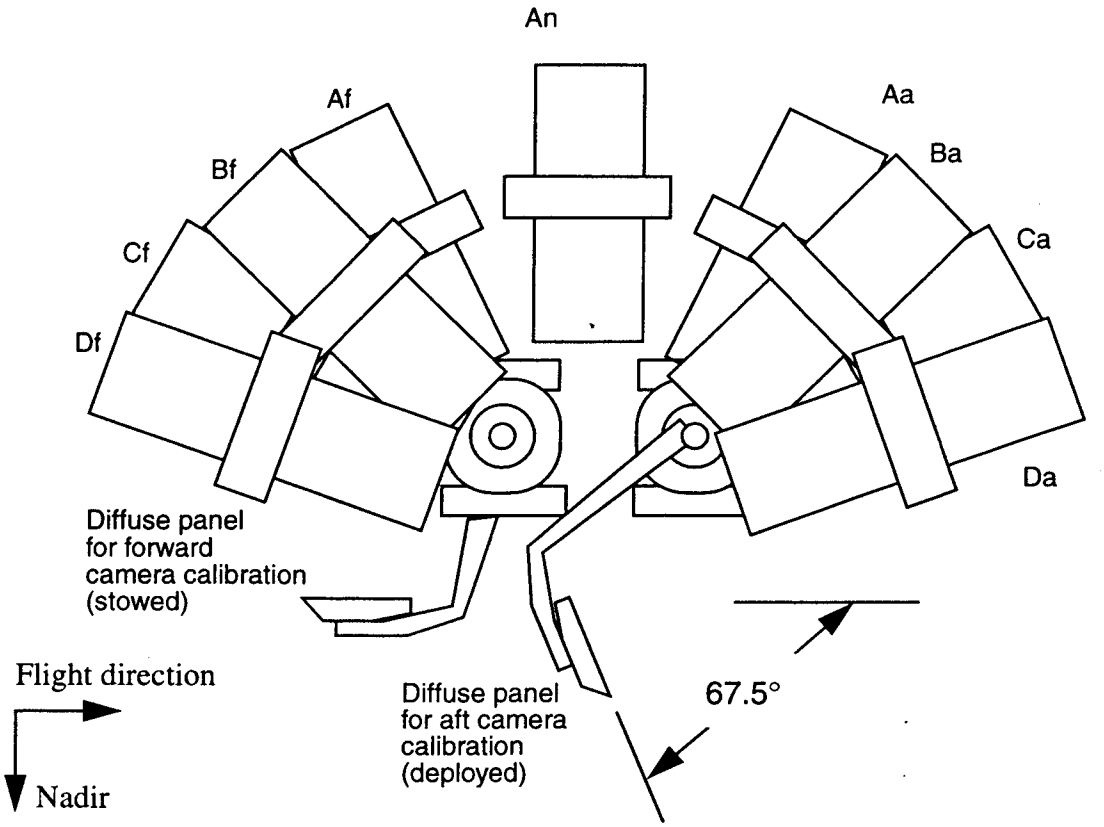

Figure 1. Diffuse panel deployment for MISR in-flight calibration.

Six sets of detector standards are used to monitor the radiance reflected from these panels, with each set consisting of four photodiodes filtered to the four MISR spectral passbands. The photodiodes are of two basic designs. Five such sets are single photodiodes, termed PIN photodiodes. These are mounted at two nadir-viewing positions, at the Da and Df camera viewing positions, and on a goniometer which swings at ±65° along the flight direction. An additional photodiode set is constructed in a light trap configuration, and uses High Quantum Efficiency (HQE) photodiode technology. The HQE photodiodes are nadir-viewing. As the photodiodes have a field-of-view of 2.5°, and the cameras have a cross-track field of view as large as ±14.9° (for the A-designed lens), the photodiodes do not measure light reflected in all of the A and D angle view directions. Nor are there photodiodes in the B or C viewing angle directions. Thus, the panel BRF is used to determine these radiance values for angles in which the radiance is not directly measured. This is provided by the relationship

$$L^{p}(\theta_i;\theta_r^{p},\phi_r^{p}) = L^{OBC}(\theta_i;\theta_r^{OBC},\phi_r^{OBC}) \cdot \frac{R(\theta_i;\theta_r^{p},\phi_r^{p})}{R(\theta_i;\theta_r^{OBC},\phi_r^{OBC})} \tag{12}$$

Here L^{OBC} and L^{p} are radiances incident onto the OBC photodiodes and CCD pixels, p, respectively. These radiances are computed at the four MISR spectral bands.

During on-orbit calibration, data are acquired simultaneously with the photodiode detector standards, and the CCD cameras. This occurs throughout a five minute window, during which the sun transits a range of solar illumination and azimuth angles. These angles are shown in Figure 2, where here the illumination angles are defined with respect to the panel coordinate system. That is, ϕ_p=0° for illumination along the spacecraft -y axis, and θ_p=0° for illumination along the panel normal. The expected range of view elevations from the MISR cameras is 9° to 70°. The anticipated solar incidence angle onto the calibration panels is from 38° to 55°, as measured from the surface normal.The azimuth angles relative to the source (which corresponds to our laboratory setup) will be on the ϕ_r = 180° side.

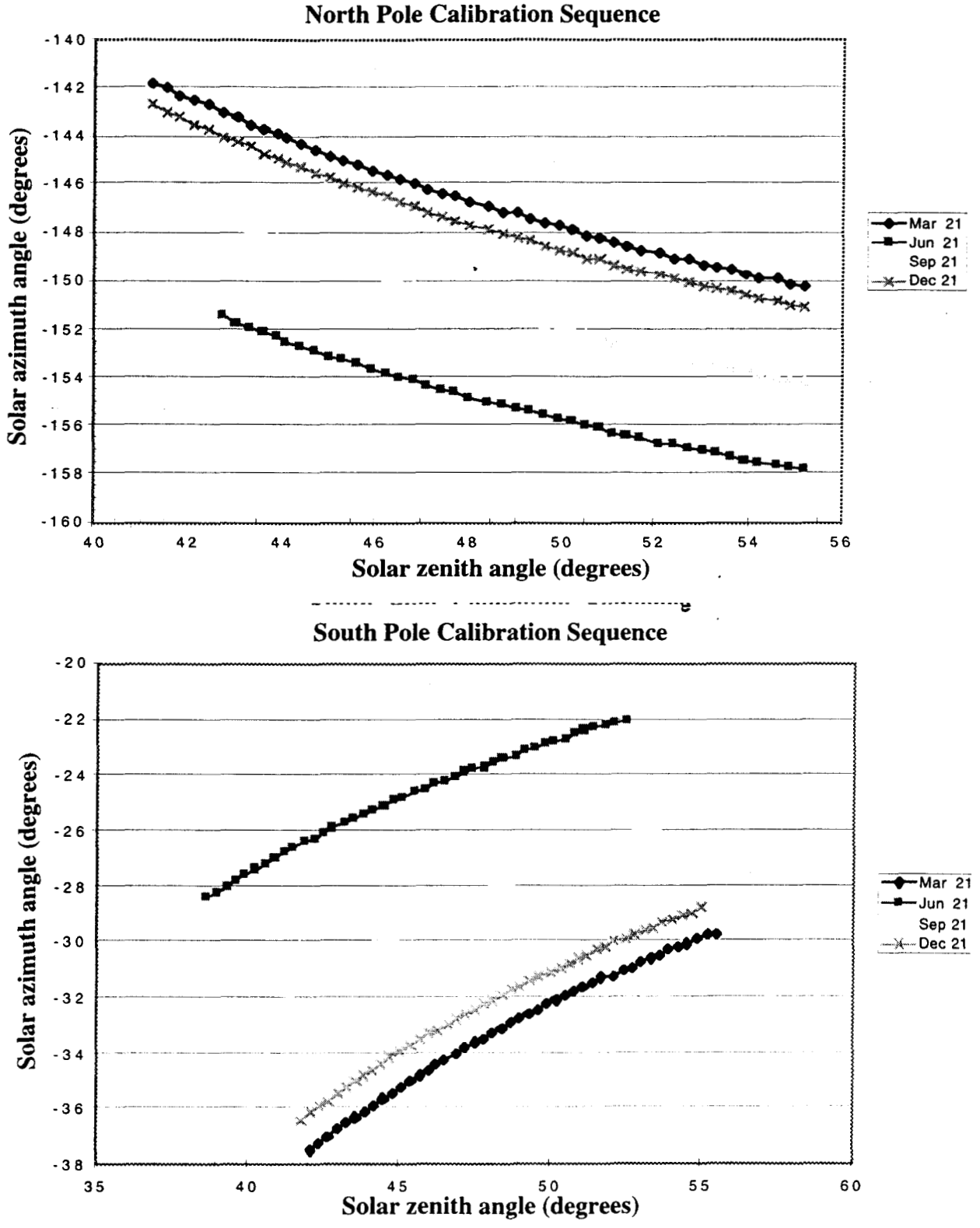

Figure 2. Solar angles onto the diffuse panel during the North and South pole panel deployments.

Vicarious calibration

In addition to assigning a radiometric calibration to the instrument via the OBC, MISR will make use of vicarious calibration (VC) methodologies. Using a desert playa, such as Lunar Lake, the surface BRF, $R_{targaet}(\theta_i;\theta_r,\phi_r)$, will be characterized both spatially and with view angle. This will be done using spectrally filtered radiometers, ratioing instrument output voltage to that of a Spectralon reflectance standard. A description of the VC radiometers is found in Abdou et al. (1999) For these field applications, knowledge of the panel HDRF is required. Given this to be known, the surface reflectance is retrieved via the following formalism:

$$r_{target}(2\pi;\theta_r,\phi_r)=V_{target}(2\pi;\theta_r,\phi_r)\, r_{standard}(2\pi;\theta_r,\phi_r)/\, V_{standard}(2\pi;\theta_r,\phi_r) \qquad (13)$$

From such a measure of the surface HDRF through a range of varying solar illumination angles, the surface BRF can be retrieved (1999). Knowledge of the Spectralon standard HDRF is not easily obtained. For a nadir viewing sensor and clear atmospheric conditions, it can be approximated from the BRF. For more general conditions the more exacting approach is needed, as is discussed in the section on Spectralon HDRF determindation.

SPECTRALON BRF DATA ACQUISITION

Experimental set-up

Details of the facility used to characterization the Spectralon panels has been described elsewhere (McGuckin, et al., 1996), but will be briefly summarized here. A simplified schematic of the set-up is shown in Figure 3. Laser illumination was chosen for this experiment. This decision was made in order to fulfill the requirement to measure relative BRF to within 0.1% precision. The intensity provided by these laser sources allowed detection to be made with high signal-to-noise. As Spectralon reflectance properties are known to be a slowly varying function of wavelength, the use of broadband illumination or detection was not a priority. Three laser sources were utilized, each within ±5 nm of a MISR spectral band. These sources were a helium cadmium (HeCd) laser at 442 nm, a helium neon laser (HeNe) at 632.8 nm, and a gallium aluminum arsenide (GaAlAs) semiconductor diode laser source at 859.9 nm. Although a convenient source was not found to measure the 558 nm band, the existing sources do allow coverage of the MISR extreme wavelength range.

Commercially available rotation stages control the detector and target rotation. Each is capable of 360° rotation with 0.05° accuracy. A cradle is used to position the target elevation angle, moving ±45° in travel. Care is taken to insure all rotations are made using an axis that is on the front surface of the panel to be characterized. The set-up was built to completely characterize a target between 1 and 4" square, or to provide principal plane (only) viewing angles of the 52.2 x 7.1 x 0.71 cm (20.6 x 2.8 x 0.28") flight target. The flight target is too large to be rotated out-of-plane, as it would collide with the optical bench table.

The relative amplitude of the light incident upon the Spectralon panel is controlled by a zero-order half-wave plate and polarizer combination. The latter was orientated to pass either s- or p-

polarized light relative to the plane containing the detector and the incident beam, termed the principal plane. Scattered light is measured unpolarized, as MISR is a polarization insensitive instrument. A reference detector continually monitors the illumination, in order to account for amplitude fluctuations of the source. Both the panel-viewing and reference detectors use 1-cm square silicon photodiodes. Each detection channel uses phase-sensitive detection and amplification, and a 16-bit analog-to-digital (A/D) converter. A personal computer is used for data acquisition and processing.

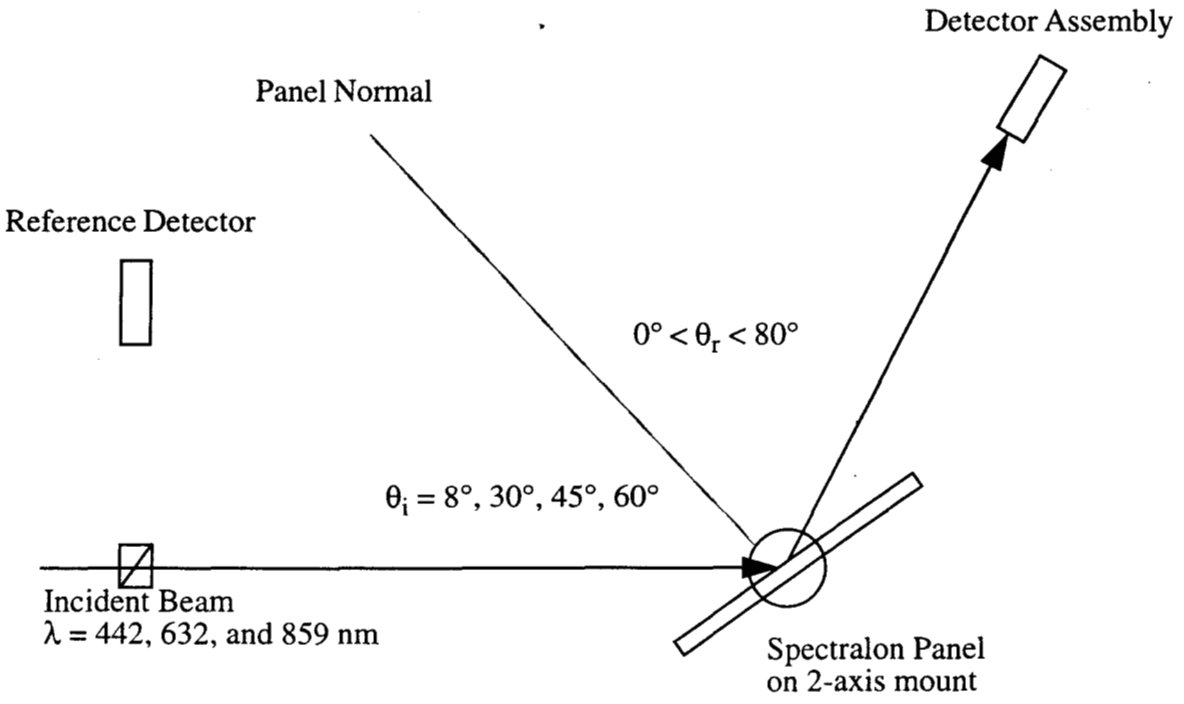

Figure 3. Optical layout of the BRF test facility

Experiment plan

The full-hemisphere BRF measurements were performed on test-pieces, as the laboratory setup did not allow such measurements to be done on the actual flight units. These test pieces were manufactured simultaneously with the flight panels, as each was cut from the same tile. Packing density, baking, and sanding histories were identical, and thus test-piece BRF data were acquired to serve as proxy for flight hardware reflectance values.

Based upon the viewing geometries depicted by Figure 2, the measurement plan elected was to provide data acquisition at illumination angles of 40°, 45°, 50° and 55°. In addition, an illumination of 8° was provided in order to make a verification of the BRF scale, by comparison with the DHR provided with the targets by the vendor. (Recall DHR was defined by Eqn. (11)). The sampling strategy for the reflected light was such that an integration of the directional values would allow DHR computation. For each angle of incidence, the detector viewed the reflected

signal at elevation angles of 1°, 10°, 20°, 30°, 40°, 50°, 60°, 70° and 80° and azimuth angles from 0° to 180° at a sampling interval of 10°. Symmetry in the BRF distribution for azimuth angles from 180° to 360° was assumed.

Data reduction

The MISR reflectance data consist of two measurements: the incident signal, V_i , and the reflected signal, V_r.

$$R(\theta_i;\theta_r,\phi_r) = \left[\frac{V_r(\theta_r,\phi_r)}{V_{r,\,ref}(\theta_r,\phi_r)}\right] \Big/ \left\{\left[\frac{V_i(\theta_i)}{V_{i,\,ref}(\theta_i)}\right] \cdot \Omega_d 10^{ND} \cdot \cos\theta_r\right\} \tag{14}$$

where Ω_d is the detector solid angle, 10^{ND} refers to the neutral density filter used in calibration, and $V_{i,ref}$ and $V_{r,ref}$ are values of the incident and reflective beams, as acquired by the reference detector. Table 2 gives the spectral constants for this experiment.

Table 2. Experimental parameters

λ, nm	Ω_d , sr	10^{ND}
442	8.722e-4	3.126e3
632	8.722e-4	2.838e3
860	8.722e-4	4.074e3

Measurements are taken for both s-polarization incident and p-polarization incident illumination conditions. These data are then converted to BRF that for an unpolarized source by taking the average of the s-polarization incident and p-polarization incident BRFs:

$$R_{unpol}(\theta_i;\theta_r,\phi_r)=[R_s(\theta_i;\theta_r,\phi_r) + R_p(\theta_i;\theta_r,\phi_r)]/\,2\,. \tag{15}$$

The measured BRF was resampled via spline interpolation/extrapolation and a numerical integration over the hemisphere was performed to arrive at the DHR (see Table 3). Specifically, a second-order polynomial fit to the data was done in the θ_i dimension, and a spline fit was done in each of the θ_r and ϕ_r dimensions. The DHR (interpolated to 632 nm) measured by Labsphere for a source at 8° for the same sample was 0.983, a 0.8% difference from our result. Some discrete values of the BRF are given in Tables 3 and 4.

For processing of on-orbit data, MISR has resampled the measured BRF data to 2° intervals throughout the hemisphere. A linear interpolation is then used to find illumination and view angle specific values.

Table 3. BRF for a nadir viewing sensor and DHR values at 632.8 nm. Data were acquired at 632.8 nm and varying illumination angles.

Illumination, θ_i	BRF $R(\theta_i;0°)$	DHR $\rho(\theta_i;2\pi)$
8°	1.045	0.991
40°	1.004	0.990
45°	0.994	0.993
50°	0.983	0.983
55°	0.972	0.990

Table 4. BRF at MISR view angles, 45° incident angle, and 632.8 nm illumination.

Camera name	View angle, θ_r	BRF, $R(45°;\theta_r,\phi_r)$ vs. view azimuth, ϕ_r				
		0°	45°	90°	135°	180°
An	0°	0.995	0.995	0.995	0.995	0.995
Af/ Aa	26.1°	0.982	0.985	0.995	1.010	1.020
Bf/ Ba	45.6°	0.970	0.967	0.988	1.021	1.047
Cf/ Ca	60.0°	0.926	0.945	0.979	1.027	1.069
Df/ Da	70.5°	0.886	0.918	0.968	1.030	1.093

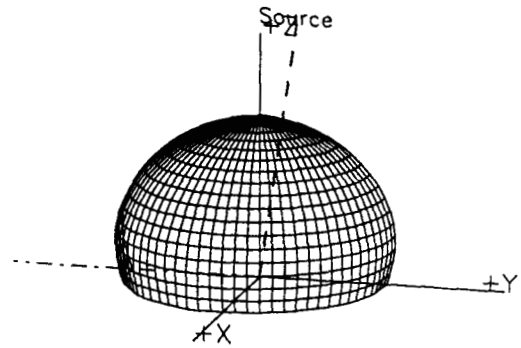

(a) θ_i=8°

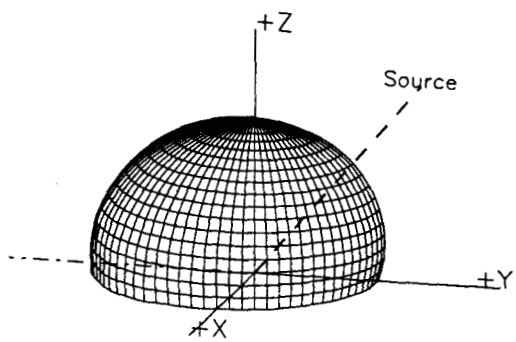

(b) θ_i=40°

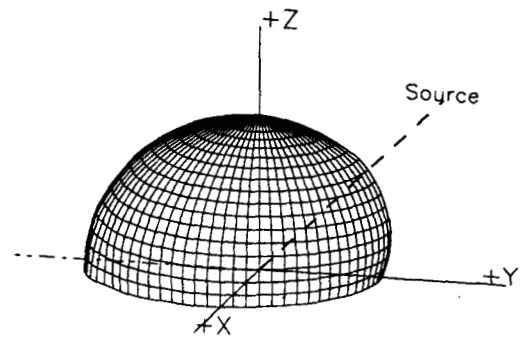

(c) θ_i=45°

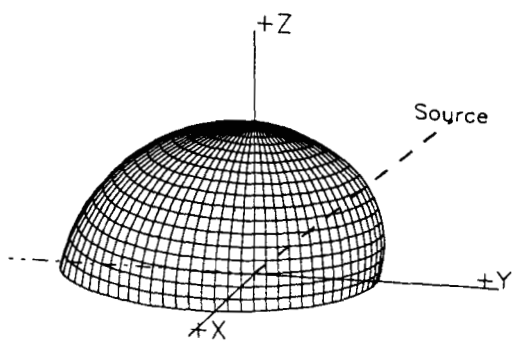

(b) θ_i=50°

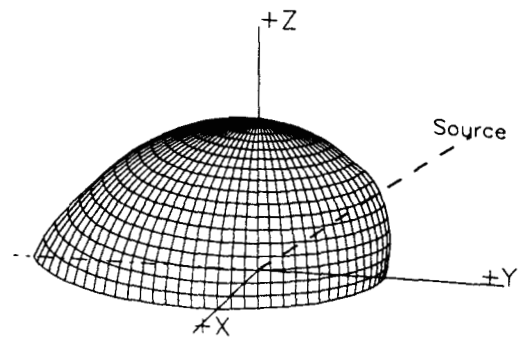

(b) θ_i=55°

Figure 4. Measured hemispheric BRF of test-piece 12669-2 at 632.8 nm.

SENSITIVITY STUDIES

Polarization

Figure 5 shows the differences in the reflectance of Spectralon for s- and p-illumination conditions. It is the average of these data that are used to construct the BRF appropriate for unpolarized illumination. It is the unpolarized BRF that is applicable to our calibration applications. A further study on differences in reflectance properties with polarization is provided by Haner et al. (1999).

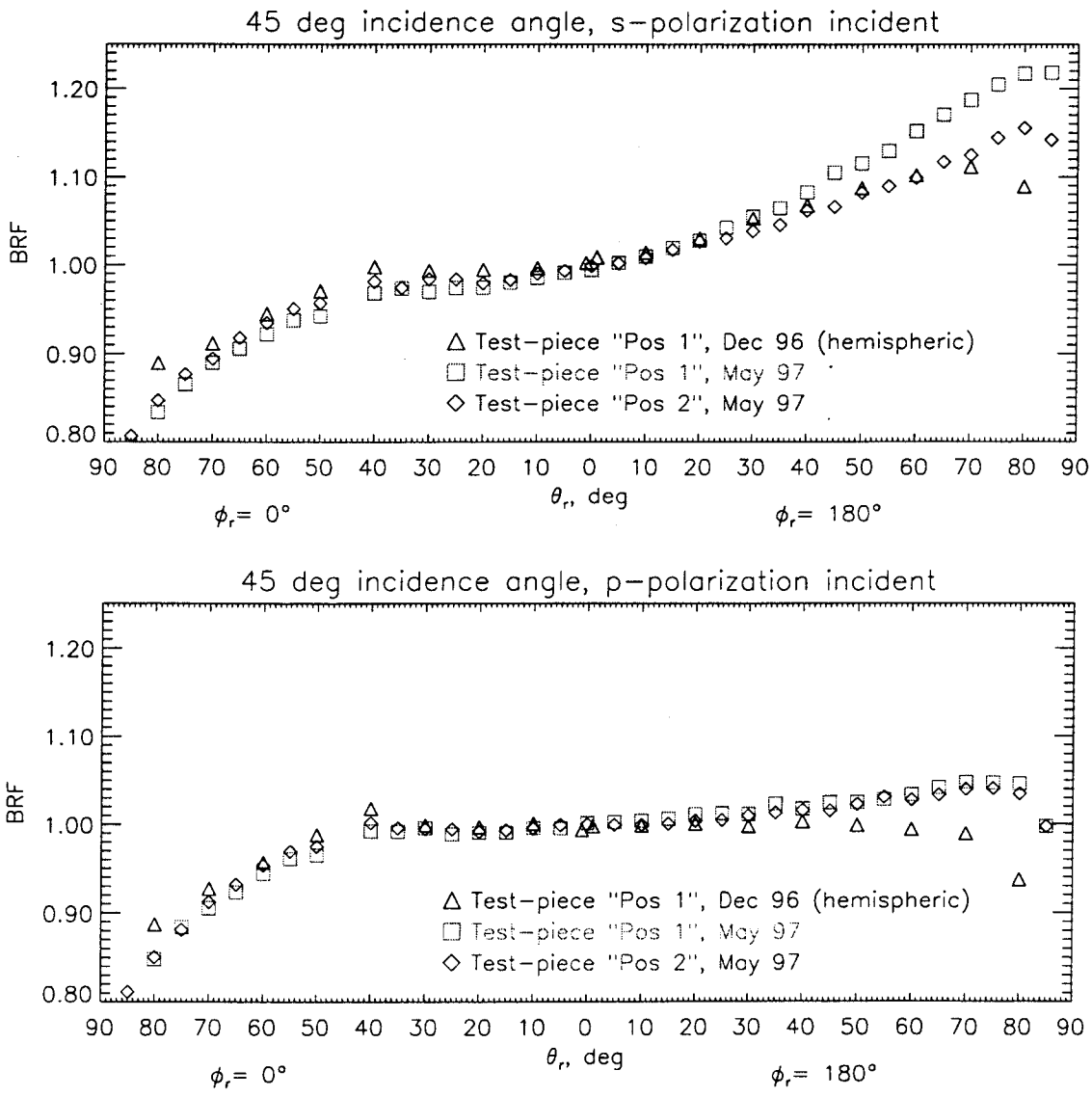

Figure 5. BRF components for s- and p-incident light.

Wavelength

Comparisons of the principal-plane BRF data at 632.8 nm with that acquired at 442 and 860 nm are shown in Figure 6. Peak-to-peak differences are found to be as large as 2.5%, with a standard deviation of 1%. We believe this uncertainty to be within the precision of the measurements.

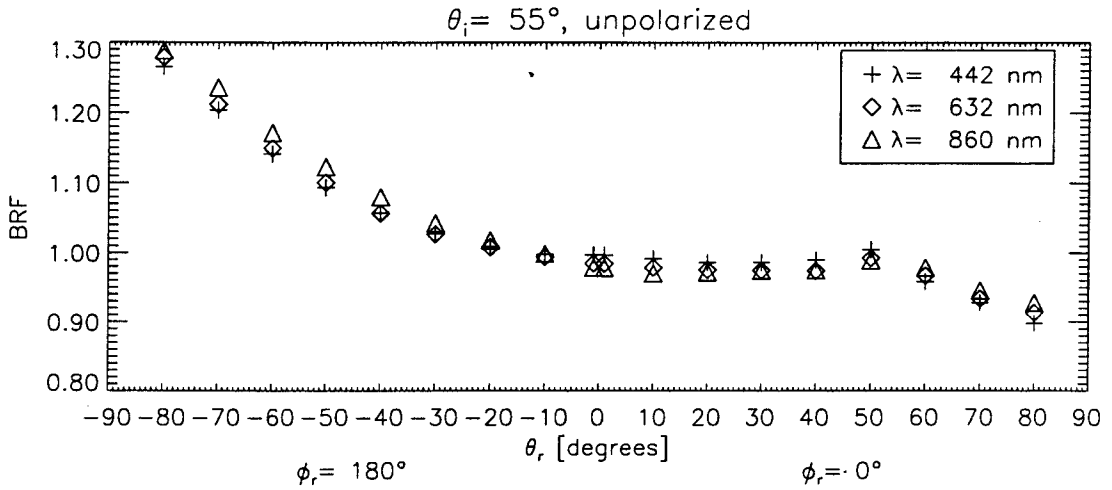

Figure 6. Principal plane BRF with wavelength.

Target/ target differences

Figure 7 shows a comparison of the BRF in the principal plane for both the test piece and flight panels. During this study it was discovered that the test-piece had two distinct regions to it. Rotation of the test-piece by 90° in the laboratory measurement setup did not affect the result. The flight panels, which are much longer than the test-piece, exhibited greater spatial uniformity in the BRF. It was subsequently noted that there was a slight dip in the test-piece in the vicinity of Position 1, which is visually barely noticeable. As shown in the figure, data acquired at test-piece Position 2 better matched the BRF results obtained from the flight units. The data from this position

are the ones delivered for MISR in-flight calibrations and are referred to as "the Spectralon BRF database".

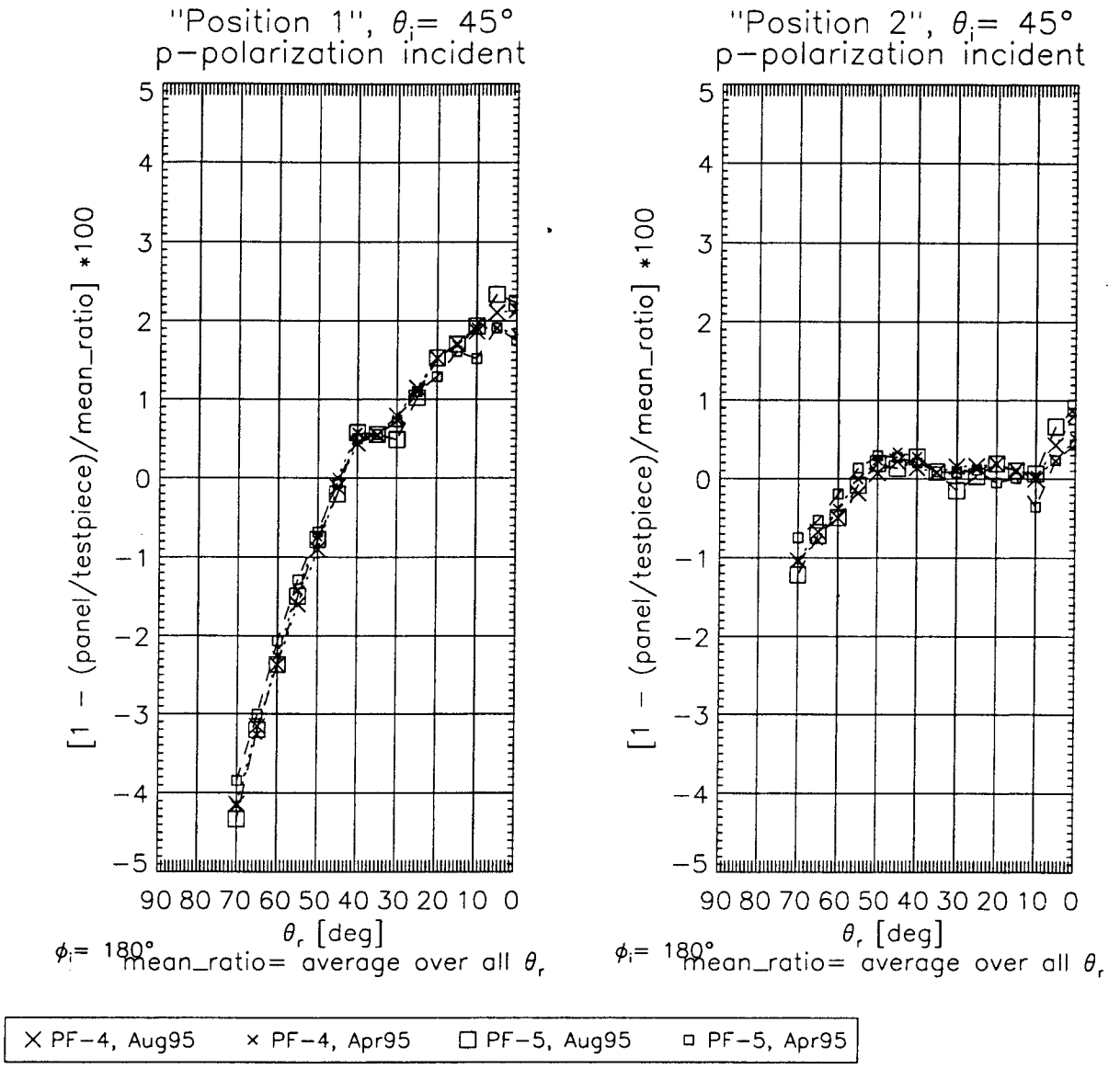

Figure 7. Relative difference between flight panels and test-piece

BRF UNCERTAINTY ESTIMATION

Experimental errors

An error analysis of the BRF values is provided in Table 5. The values for the two largest error sources, that of the panel uniformity and wavelength variability, are motivated from studies such as that described above. Other sources of error are not precisely known, but are thought to be negligible (McGuckin, et al., 1997), and are written here with an over estimation of 0.05. We see that our uncertainty in relative BRF is large (1.4%), but sufficient to achieve a 3% absolute

calibration. The camera-relative and band-relative calibration requirements will only be met if panel uniformity and wavelength variability are in practice less that the conservative estimates given here. It is for these reason that the MISR OBC may best be viewed as determining the absolute radiance scale for the cameras, and that multiple calibration methodologies remain important to the MISR program. Camera-relative calibrations will accurately be made using AirMISR (a single-camera instrument gimbaled to the MISR angles), and histogram equalization techniques (using a statistical compilation of Earth observations). This method will supplement the OBC relative calibration.

Table 5. BRF error sources

Error source	Error in relative BRF, %	Error in absolute BRF, %
Panel uniformity	1	1
Wavelength variability	1	1
Panel thickness	0.05	0.05
Laser speckle	0.05	0.05
Goniometer positional accuracy	0.05	0.05
Detector SNR	0.05	0.05
Detector linearity	0.05	0.05
Filter transmittance knowledge	Not applicable	1
Root-sum-square total	1.4	1.7

Data validations

In addition to the error analysis described above, several data validation exercises were carried out. These studies are summarized in the matrix provided in Table 6.

Table 6. Spectralon BRF validation study matrix

Study name	Parameter, illumination angle, θ_i, and wavelengths compared	Sample measured by JPL	Comparison sample	Results
EOS-RR	principal-plane BRF at 30°, 45°, and 60°	NIST provided	Same target	Agreement within 0.5%.

Table 6. Spectralon BRF validation study matrix

Study name	Parameter, illumination angle, θ_i, and wavelengths compared	Sample measured by JPL	Comparison sample	Results
RIT	principal-plane BRF at 45° (hemispheric data available)	Test-piece[a]	Unrelated sample	Agreement to within 5% for view angles to 30°, 15% differences in the forward scattered direction for larger angles.
TMA	principal-plane BRF at 45° and 632 nm	Test-piece[a]	Unrelated sample	Agreement is within 1% for view angles to 60° and 5% to 70°
Model	hemispheric BRF at 632 nm	Test-piece[a]	Unrelated sample	1-5%
Labsphere	DHR at 8°, 632 nm	Test-piece[a]	Same target	Agreement within 0.8%

a.This is the same test-piece as was used to develop the MISR BRF database, serial number 12669-2.

These studies were:

- EOS-RR: a comparison of BRF as acquired during an EOS round-robin experiment (Barnes, et al., 1998; Early, et al., 1999). Agreement with the National Institute of Standards and Technology (NIST) was excellent, verifying our data methodology and data reduction procedures.
- RIT: a comparison of our full-hemisphere Spectralon BRF database to that reported by the Rochester Institute of Technology (Feng, et al., 1993) was made. Differences were larger than other comparisons, however sample differences are possible;
- TMA: a comparison of our principal-plane Spectralon BRF database to that reported by TMA technologies showed excellent agreement though different samples were measured;
- Model: a comparison of our full-hemisphere Spectralon BRF database to a Spectralon model reported in the literature (Flasse, et al., 1993). The model was generated using the principal-plane TMA data. Differences might have been smaller had the model been developed using the test-piece hemispheric BRF data;
- Labsphere: a comparison of our integrated DHR values to those reported by Labsphere showed good agreement.

The most definitive verification of our data accuracy comes from the EOS round-robin experiment. Here common samples were measured at the respective facilities. With agreement within 0.5%, this study supports our BRF uncertainty estimates provided in Table 5. Note that our error estimate is larger than differences shown by the EOS-round-robin experiment. This is due to

the fact that for the round-robin no wavelength extrapolation was required, and the same panel and position within the panel was measured.

SPECTRALON HDRF DETERMINATION

For field applications, such as vicarious calibration, panel reflectance must be known for the specific diffuse plus solar/ direct irradiance conditions present at the moment the panel is measured. As this HDRF varies temporally with changing solar angle and with atmospheric conditions, it is difficult to determine. For clear atmospheric conditions, particularly at the longer wavelengths, it may be approximated by the BRF. The accuracy of this approximation has been detailed in the literature. An excellent discussion of this problem is given, for example, in Gu and Guyot (1993). These authors make the observations that:

- wavelength and atmospheric visibility effect HDRF through changes in the diffuse to direct surface irradiance;
- for an isotropic distribution of the surface irradiance, the HDRF (directional in view angle) is numerically equivalent to the DHR (directional in illumination angle) due to Helmholtz recriprocity principle;
- for direct only illumination the HDRF is equivalent to the BRF;
- the HDRF for any arbitrary field condition lies between the BRF and the DHR of the surface;
- differences in BRF and DHR are minimal for a reflectance standard that approaches Lambertian behavior.

Although these general observations are applicable to the MISR off-nadir views, their analysis is specific to the nadir-view case. For example, for this case only knowledge of the azimuthal average of the BRF and irradiance conditions. Conversely, for off-nadir views the complete integral provided by Eqn. (10) must be considered. In practice the MISR vicarious calibration analysis wll only require reference to the standard in a nadir-view configuration. This is because the relative multi-angle views of the Earth surface's can be scaled to an absolute reflectance by normalization to the standard at the nadir-view case. However, knowledge between differences in HDRF and BRF for the more general case are of interest from the perspective of considering optional methodologies and procedures.

As Spectralon diffusers do indeed approach Lambertian behavior, particularly for small solar incident angles, we would like to validate that the HDRF can be approximated as the BRF. This assumption would not normally be made for arbitrary surfaces, or diffusers not as Lambertian as Spectralon. We estimate the error here, for a range of atmospheric conditions and solar angles. This is done by assuming, for any a real atmosphere, the differences in these two functions fall somewhere between the direct beam (E_{dif}=0) case and the isotropic diffuse irradiance condition with a known E_{dif}/E_{tot} ratio. Making use of Eqn. (10) with the isotropic assumption, we have

$$r(2\pi;\theta_r,\phi_r) = R(\theta_i;\theta_r,\phi_r)\cdot E_{dir}/E_{tot} + \rho(\theta_r;2\pi)\cdot E_{dif}/E_{tot}$$

$$= R(\theta_i;\theta_r,\phi_r)(1 - E_{dif}/E_{tot}) + \rho(\theta_r;2\pi)(E_{dif}/E_{tot}) \qquad (16)$$

The results of such a study is presented in Figure 8, for a range of solar elevation angles and the MISR camera view angles. For simplicity a single azimuthal view angle of 135° is selected. In order to compare these E_{dif}/E_{tot} ratio cases to specific atmospheric conditions, the data values published in Gu and Guyot, and shown in Table 7, are referenced. We note that in the limiting case of direct beam illumination the HDRF is identically equal to the BRF. For an extreme case of diffuse only illumination (E_{dir}=0), the HDRF would be equal to the DHR. A more realistic worst-case diffuse illumination is that depicted in the figure, E_{dif}/E_{tot}=0.6. For this computation a DHR of 0.99 was assumed, consistent with the findings reported in Table 3.

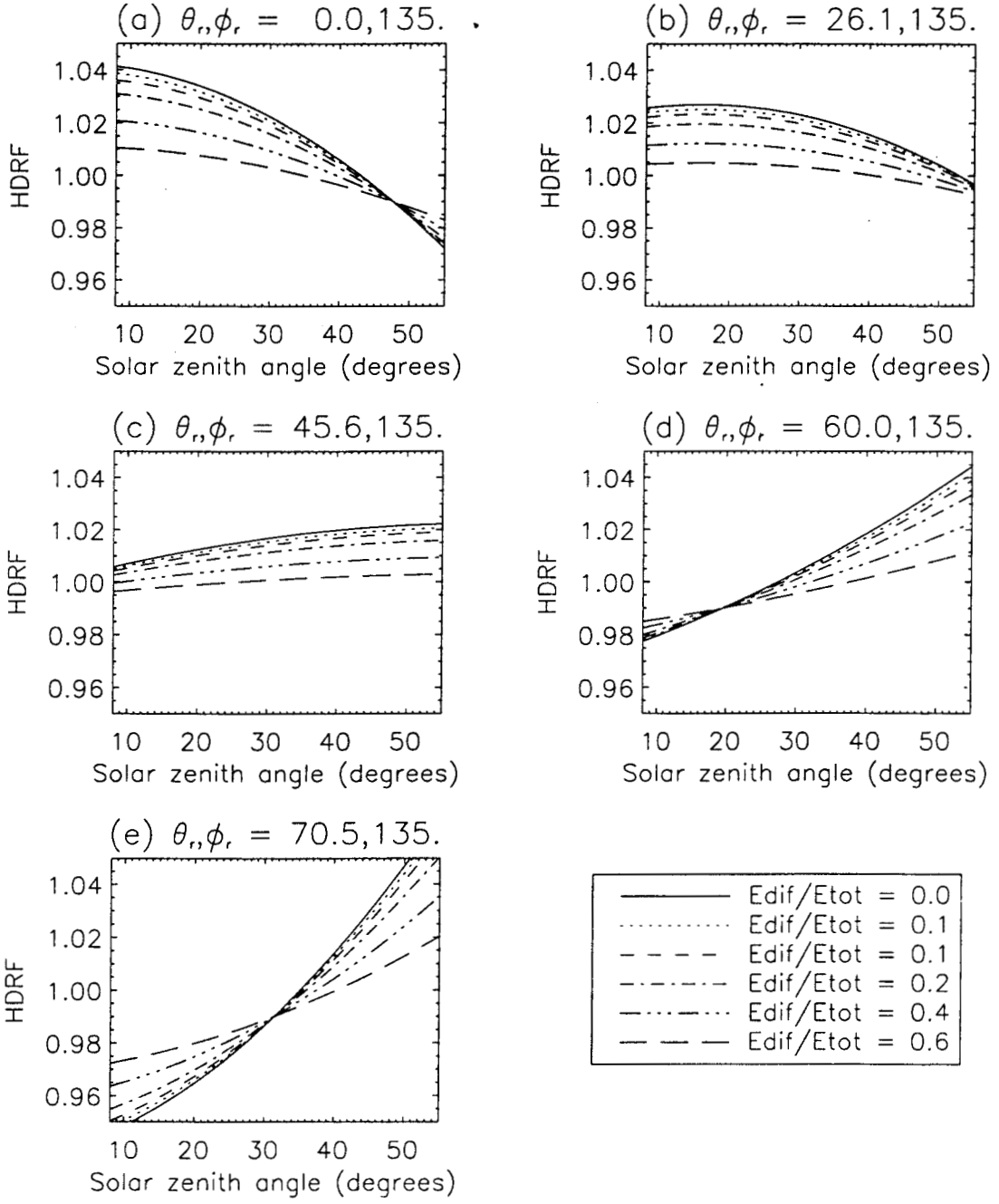

Figure 8. Variations in HDRF for various E_{dir}/E_{tot} irradiance conditions. Plots (a) through (e) give results for MISR cameras An through D, respectively.

By inspection of Eqn. (16) it is seen that the ratio E_{dir}/E_{tot} can be solved for directly, given an acceptable tolerance in HDRF versus BRF. This is given as

$$E_{dif}/E_{tot}(\theta_i;\theta_r,\phi_r) = \frac{R(\theta_i;\theta_r,\phi_r) \cdot \text{tolerance}}{R(\theta_i;\theta_r,\phi_r) - \rho(\theta_i;2\pi)} \tag{17}$$

Results of this study are presented in Figure 9. By comparing these results to that of Table 7, we see that the BRF approximation is valid, provided the atmosphere is reasonably clear. These conclusions could not had been made, had the Spectralon not been sufficiently Lambertian.

Table 7. Diffuse to direct ratios versus visibility at 550 nm

θ_o (degrees)	E_{dir}/E_{tot} versus visibility (km)		
	10	50	999
25.1	0.39	0.19	0.053
47.3	0.46	0.23	0.72
65.9	0.63	0.34	0.12

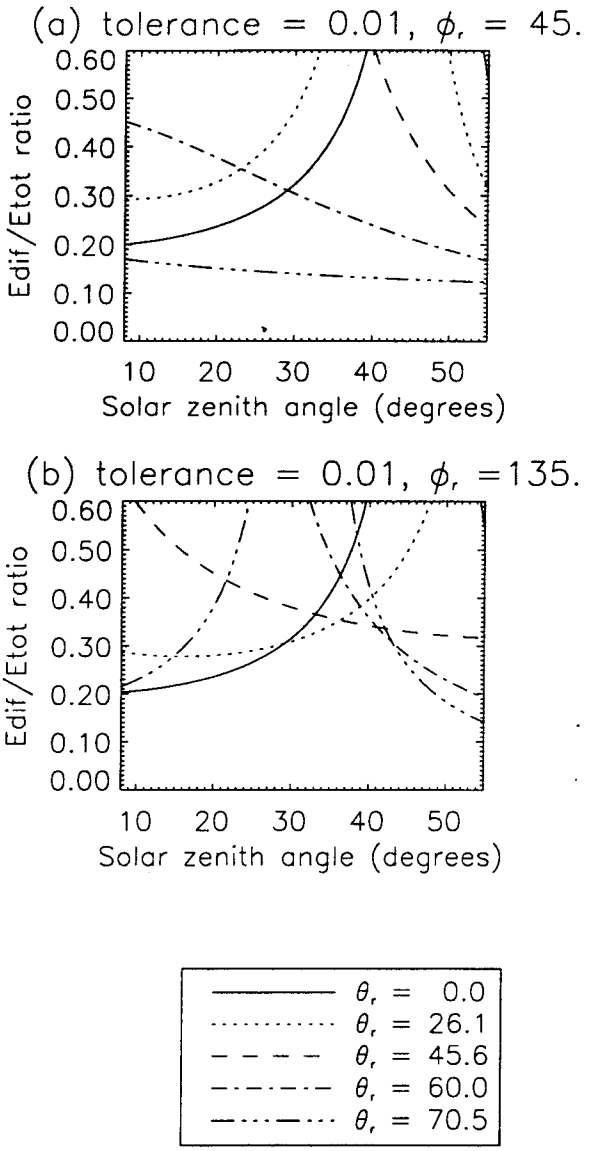

Figure 9. Upper bound on $Edir/E_{tot}$ required to achieve HDRF and BRF agreement within a tolerance of 0.01. Figures (a) and (b) give examples for two view azimuths.

CONCLUSIONS

The MISR team has developed a Spectralon BRF data base for use in its on-board and vicarious calibration experiments. Care has been taken to investigate the generality of the BRF from panel to panel or positions within a panel, and to understand its dependence on wavelength. We believe that the BRF measured here at 632 nm is representative of any high quality panel to

within 1% (to view angles out to 50°), or to within 2% for view angles out to 70°. This uncertainty will allow us to meet our absolute radiometric calibration requirement of 3%. The camera- and band-relative calibrations will be more challenging with this approach. It is for this reason that MISR also makes use of other calibration methodologies, such as the response determined from compiling Earth scene statistics (histogram equalization) and AirMISR underflights.

The potential for on-orbit degradation of the BRF is not addressed here. A previous study (Bruegge, et al., 1991) has indicated that the BRF is invariant upon panel yellowing. To monitor this assumption, MISR has incorporated a goniometer within the OBC. Should a change in the BRF profile be measured, the uncertainty in the radiometric calibration would increase.

For field applications, the diffuse/ direct ratio of solar illumination can be used to validate the assumption of using the Spectralon BRF as an approximation to the HDRF.

ACKNOWLEDGMENTS

Art Springsteen of Labsphere, Inc. is to be thanked for providing many of the references and comparison data sets quoted here, and for his many helpful discussions. Yvonne Barnes and Ted Early of the National Institute of Standards and Technology are to be thanked for conducting the EOS round-robin BRF comparison experiment. The TMA data used in the validation study were supplied by Jim Irons, Goddard Space Flight Center. David Haner is also affiliated with the California State Polytechnic University, Pomona, California. The work described in this paper is being carried out by the Jet Propulsion Laboratory, California Institute of Technology, under contract with the National Aeronautics and Space Administration.

REFERENCES

Abdou, W.A., C.J. Bruegge, M.C. Helmlinger, B.J. Gaitley, W.C. Ledeboer, S.H. Pilorz, J.E. Conel, and J.V. Martonchik (1999), Vicarious reflectance-based absolute radiometric calibration of AirMISR, *Remote Sens. of Environment*, this issue.

Barnes, P. Yvonne, Edward A. Early, B. Carol Johnson, James J. Butler, Carol J. Bruegge, Stuart Biggar, Paul R. Spyak, and Milutin Pavlov (1998), Intercomparisons of reflectance measurements, in Proc. SPIE 3425, Optical Diagnostic Methods for Inorganic Transmissive Materials, San Diego, 20-21 July.

Bruegge, C.J., V.G. Duval, N.L. Chrien, and D.J. Diner (1993), Calibration Plans for the Multi-angle Imaging SpectroRadiometer (MISR), Metrologia, **30** (4), 213-221.

Bruegge, Carol J., Albert E. Stiegman, Daniel R. Coulter, Robert R. Hale, David J. Diner, and Arthur W. Springsteen (1991), Reflectance stability analysis of Spectralon diffuse calibration panels, in Calibration of Passive Remote Observing Optical and Microwave Instrumentation, SPIE Vol. 1493, Orlando, Florida, 3-5 April.

Bruegge, C.J., A.E. Stiegman, R.A. Rainen, A.W. Springsteen (1993), Use of Spectralon as a diffuse reflectance standard for in-flight calibration of earth-orbiting sensors, Opt. Eng. **32**(4), 805-814.

Diner, D.J., J.C. Beckert, T.H. Reilly, C.J. Bruegge, J.E. Conel, R. Kahn, J.V. Martonchik, T.P. Ackerman, R. Davies, S.A.W. Gerstl, H.R. Gordon, J-P. Muller, R. Myneni, R.J. Sellers, B. Pinty, and M.M. Verstraete (1998), Multiangle Imaging SpectroRadiometer (MISR) description and experiment overview, IEEE Trans. Geosci. Rem. Sens., Vol. 36, 1072-1087.

Early, E.A., P.Y. Barnes, B.C. Johnson, J.J. Butler, C.J. Bruegge, S. Biggar, P.R. Spyak, and M.M. Pavlov (1999), Bidirectional reflectance round-robin in support of the earth observing System program, in preparation for submission to J. Atmos. and Oceanic Tech.

Feng, Xiaofan, John R. Schott, and Timothy Gallagher (1993), Comparison of methods for generation of absolute reflectance-factor values for bidirectional reflectance-distribution function studies, Appl. Opt. 32(7): 1234-1242.

Flasse, S.P., M.M. Verstraete, B. Pinty, and C.J. Bruegge (1993), Modeling Spectralon's bidirectional reflectance for in-flight calibration of Earth-orbiting sensors, In Recent Advances in *Sensors, Radiometric Calibration, and Processing of Remotely Sensed Data*, Proc. SPIE **1938**, April, 100-108.

Gu, Xing-Fa, and Gérard Guyot (1993), Effect of diffuse irradiance on the reflectance factor of reference panels under field conditions, Remote Sens. Environ. 45:249-260.

Haner, D., B.T. McGuckin, and C.J. Bruegge (1999), Polarization characteristics of Spectralon illuminated by coherent light, in preparation for submission to IEEE Trans. Geosci. Rem. Sens.

Jackson, Ray D., Thomas R. Clarke, and M. Susan Moran (1992), Bidirectional calibration results for 11 Spectralon and 16 $BaSO_4$ reference panels, Remote Sens. Environ. 40: 231-239.

Labsphere, Inc. (1998), Reflections Newsletter, pp. 1-4, September.

Martonchik, J.V. (1994), Retrieval of surface directional reflectance properties using ground level multi-angle measurements, Remote Sens. Environ., 50: 303-316.

McGuckin, B.T., D.A. Haner, R.T. Menzies, C. Esproles, and A.M. Brothers (1996), Directional reflectance characterization facility and measurement methodology, Appl. Opt. 35(24), pp. 4827-4834.

McGuckin, Brendan T., David A. Haner, and Robert T. Menzies (1997), Multiangle Imaging SpectroRadiometer: optical characterization of the calibration panels, Appl. Opt. 36(27), pp. 7016-7022.

Meyer-Arendt, J.R. (1968), Radiometry and photometry: units and conversion factors, *Appl. Opt.* **7**:2081-2084.

Nicodemus, F.E., J.C. Richmond, I.W. Ginsberg, J.J. Hsia, and T. Limperis (1977), Geometrical considerations and nomenclature for reflection, National Bur. Stand. U.S. Monogr. 160.

Stiegman, A.E., C.J. Bruegge, A.W. Springsteen (1993), Ultraviolet stability and contamination analysis of Spectralon diffuse reflectance material, Opt. Eng. **32**(4), 799-804.

Sümnich, K.H., A. Neumann, H. Schwarzer, T. Walzel, G. Zimmermann (1997), Modular optoelectronic scanner MOS in-orbit; results of the in-flight calibration, SPIE Vol. 3118, San Diego, 28-30 July.

Weidner, V.R., and J.J. Hsia (1981), Reflectance properties of pressed polytetrafluoroethylene powder, J. Optical Society of America, 71: 856-861.